Food Hydrocolloids 23 (2009) 1660–1669

Contents lists available at ScienceDirect

Food Hydrocolloids

journal homepage: www.elsevier.com/locate/foodhyd

Rheological characterization of deacylated/acylated gellan films carrying L-(+)-ascorbic acid

Paula G. León [a,1], Stefania Chillo [b], Amalia Conte [b], Lía N. Gerschenson [a,2], Matteo A. Del Nobile [b], Ana M. Rojas [a,*,2]

[a] Departamento de Industrias, Facultad de Ciencias Exactas y Naturales, Universidad de Buenos Aires, Ciudad Universitaria, 1428 Buenos Aires, Argentina
[b] Department of Food Science, University of Foggia, Via Napoli 25, 71100 Foggia, Italy

ARTICLE INFO

Article history:
Received 9 March 2008
Accepted 8 December 2008

Keywords:
Edible film
Gellan gum
Calcium
Ascorbic acid
Rheological analyses

ABSTRACT

Films developed for supporting L-(+)-ascorbic acid (AA), natural antioxidant for the protection of foods, were rheologically evaluated. A film was formulated by mixing gellan gum with its acylated form to attain a higher AA stability and lower non-enzymatic browning. The polymer mixture allowed obtaining a less rigid film, permitting the usage of a lower proportion of glycerol.

Mechanical spectra of films evidenced solid-like materials provided the time scale of the observation was shorter than the lifetime of the physical cross-links involved. There was evidence for a shorter time of relaxation in the films stored at 33.3–57.7% of relative humidity, which influenced small deformation (linear range) measurements.

Out of linear viscoelasticity a greater hardening effect was observed for A- and B-films and related to enhanced polymer interactions in gellan based films. Its increase with the moisture content may be a result of macromolecular association. Higher rigidity characterized gellan based films (A- and B-networks) at intermediate deformations, which may also lead to higher softening degree till rupture. A smaller hardening and softening degrees were observed for C- and D-systems. This can be ascribed to spatial hindering in the film network by acylated gellan chains, fact that worsened polymer interactions. Atomic force microscopy images reinforced rheological conclusions.

1. Introduction

Environmental concerns about use of non-degradable plastics for packaging and disposable consumer goods have led to intensification of the research to develop biodegradable and/or edible packaging materials (Lai & Padua, 1997). Edible film functionality has been improved and diversified through the development of different film formulations and the knowledge about them has been continuously increased due to worldwide research on their properties.

In general, polysaccharides such as pectin, starch, cellulose, alginates and other hydrocolloids, have a good performance in film-forming due to their chemical nature. (Skendi, Biliaderis, Lazaridou, & Izydorczyk, 2003). The addition of a plasticizer like glycerol or sorbitol increases the mobility of polymer chains because they reduce intermolecular forces, improving flexibility and extensibility of the film (Mali, Grossmann, García, Martino, & Zaritzky, 2005).

Acylated gellan is produced by *Sphingomonas elodea* through fermentation in culture media. Gellan (deacylated) gum is obtained further after chemical treatment for commercialization. While the acylated form produces non-brittle and elastic gels, deacylated gum yields brittle and rigid gels. The presence or absence of glicerate and acetate residues in high acyl and low acyl forms respectively, offers a wide range of textural possibilities to food technology. The addition of cations, such as calcium or potassium, increases the bond association between the film components, giving as a result, a physical cross-linked network (Chandrasekaran, Puigjaner, Joyce, & Arnott, 1988; Hamcerencu, Desbrieres, Khoukh, Popa, & Riess, 2008).

Films made from polysaccharides have good mechanical properties, but are sensitive to moisture, because of the hydrophilic nature of these components (Kristo, Biliaderis, & Zampraka, 2007). Thus, it is necessary to test their mechanical properties under different conditions of relative humidity to characterize them for future uses, taking into account consumer acceptance (Famá, Rojas, Goyanes, & Gerschenson, 2005).

* Corresponding author. Tel.: +54 11 4576 3366/3397; fax: +54 11 4576 3366.
E-mail address: arojas@di.fcen.uba.ar (A.M. Rojas).
[1] Fellow of Universidad de Buenos Aires, Argentina.
[2] Member of the National Research Council (CONICET), Argentina.

0268-005X/$ – see front matter © 2009 Elsevier Ltd. All rights reserved.
doi:10.1016/j.foodhyd.2008.12.008

Rheological properties are useful in developing structure–function relationships. Thus, the rheological analysis may provide a basic understanding about the film microstructure in relation to the composition tested (Xu, Liu, & Zhang, 2006).

As a complex matrix, food generally can not be described by an ideal model such as ideal liquid, if the matrix is viscous, or ideal solid, if it is elastic, neither as ideal plastic, a state between liquid and solid. To determine and quantify the viscoelastic behavior of a matrix, quasi-static (transient) and dynamic tests can be carried out. One of the most representative transient tests is the stress-at-break assay. It is performed by applying an increasing strain to a specimen till failure, while the stress is measured. Elastic modulus can be considered as the initial linear slope of the stress-strain curve. In dynamic tests, a sinusoidal stress or strain is applied to the specimen and the storage (shear G', or normal E') and loss (G'', or E'') moduli, as well as the tangent of the phase angle ($\tan\delta = G''/G'$, or E''/E') are measured (Del Nobile, Chillo, Mentana, & Baiano, 2007); these tests allow to acquire some knowledge about the microstructure when it is performed at linear or *at rest* conditions (scale of small deformations). A dynamic mechanical analyzer (DMA) can be used to carry out these tests evaluating the performance of different formulations (Bengoechea, Arrachid, Guerrero, Hill, & Mitchell, 2007).

In recent years, there has been an enormous demand for natural antioxidants mainly because of adverse toxicological reports on many synthetic compounds (Miková, 2001). The importance of antioxidants contained in foods is well appreciated for both preserving the foods themselves and supplying essential antioxidants *in vivo* (Shi, 2001). In this sense, edible films were formulated by using gellan polymers to support L-(+)-ascorbic acid (AA), with nutritional purposes and for natural antioxidant protection of foods (León & Rojas, 2007). The aim of the present research was the study of: (i) rheological behavior of edible films based on gellan polymers; and (ii) film microstructure in relation to composition, to provide an understanding of the influence of composition on rheological properties of films, and contribute to the optimization of their functionality.

2. Materials and methods

2.1. Materials

Food grade gellan gum (deacylated polymer; Kelcogel F) as well as its high acylated form (Kelcogel LT100) were from CP Kelco (Argentina Branch of J. M. Huber Corporation, USA). Chemicals of analytical quality were used: glycerol, L-(+)-ascorbic (AA), citric, acetic and oxalic acids, hydrogen peroxide, sodium acetate, magnesium perchlorate, sodium bromide, magnesium and sodium chloride and calcium chloride, from Anedra (Buenos Aires, Argentina), as well as potassium sorbate and 2,6-dichlorophenol indophenol from Sigma (St. Louis, MO, USA).

2.2. Preparation of films

The gellan film-forming solutions were prepared by swelling either gellan gum (for Ca-gellan system), or its mixture with the high acylated form (Kelcogel LT-100) in a 50:50 in weight proportion, into 260 g of deionized water under high speed shear (Omni-Mixer, USA), followed by heating to 90 °C at a constant heating speed on a hot plate, with simultaneous recording of the temperature every 20 s through a thermocouple connected to a Consort millivoltimeter (P 901, CE Belgium). Composition of each film-forming system solution is indicated is indicated in Table 1. Glycerol was added as a plasticizer at the indicated proportions, whereas a half of it was used for C-system. An additional formulation with the new mixture-polymer composition but with the original glycerol proportion (1 part in weight, called D) was hence elaborated and studied for comparison, expecting from its composition a considerable macromolecular mobility.

Table 1
Composition of film forming solutions.

	System solutions			
	A gellan[a]	B Ca-gellan	C	D
Gellan (Kelcogel F) (parts in weight)	1	1	0.5	0.5
Acylated gellan (Kelcogel LT 100) (parts in weight)	–	–	0.5	0.5
Ca^{2+} (mmoles)	–	2.5	–	–
Glycerol (parts in weight)	1	1	0.5	1
L-(+)-ascorbic acid (g)	0.1000	0.1000	0.1000	0.1000
Potassium sorbate (ppm)	300	300	300	300
Citric acid (g)	0.120	0.120	0.120	0.120
Deionized water, enough to	100 g	100 g	100 g	100 g
pH	3.9	3.9	3.9	3.9

[a] León and Rojas (2007).

Potassium sorbate and AA, both pre-dissolved in deionized water, were added. Glycerol was basically used at the needed proportion for film development (Yang & Paulson, 2000). Enough citric acid was added to adjust pH to a value of ≈4.0, while stirring and heating; a final pH of ≈3.8 was attained in the casted films (León et al., 2008). Calcium chloride was added to the gelling solution elaborated with gellan gum (deacylated form) after previous dissolution in deionized water, which was then called "Ca-gellan" system. The total weight of each prepared gelling solution was then made to 300.00 g by adding enough deionized water while stirring to homogenize. The hot solution was placed under vacuum to remove air-bubbles and immediately poured on to leveled glass plates. They were cooled at room temperature and then placed into an air convection-oven at 60 °C for drying. Films were peeled from the glass plates and stored at 25 °C over saturated solutions of $MgCl_2$ (water activity, $a_W = 0.333$), NaBr ($a_W = 0.577$) or NaCl ($a_W = 0.752$) till film "equilibration", which was assessed by measurement of a_W of film samples every day till attaining the RH(%)/100 (RH: relative humidity) of the saturated solution used. Afterwards, sample thickness was measured to the nearest 0.001 mm using a digital micrometer (Mitutoyo, Japan) at six different locations in each of ten specimens. Three batches of films (replicates) were prepared as indicated and stored at each relative humidity (RH) to allow considering, in the study, the influence of film making. Mechanical studies were performed in, at least, ten samples of each formulation. The following analyses were performed on samples of three batches.

2.3. NMR proton mobility

^{1}H-NMR relaxation measurements were performed on film samples using a Bruker Avance II-300 spectrometer (Germany) at 300 MHz with a Doty ^{1}H dedicated probe. The inversion-recovery sequence (p–t–p) was used to measure the spin–lattice relaxation time (T_1). A 3.6 μs of pulse duration ($p/2$) was used. The FID was exported to WIN-NMR (Bruker) software where it was Fourier transformed, phase and baseline corrected. Overlapping spectra were deconvoluted by analyses. Peak intensity (area) and line-width of the deconvoluted peaks were recorded. Curve fitting were performed at 50 and 10 μs using a non-linear fitting program (OriginPro). All analyses were performed in triplicate.

2.4. Rheological studies

2.4.1. Sample preparation

Equilibrated film samples were cut with a scalpel, into strips of 25×6 mm and left to rest for at least 24 h at the corresponding constant RH of storage, before being submitted to mechanical analyses. A gap of 14.1 ± 0.6 mm (standard deviation; $n \geq 10$) was used in the tensile experiments.

2.4.2. Normal oscillatory assay

Film sample strip was submitted to normal small amplitude strains in a cyclic manner using a dynamic mechanical analyzer DMA TA Instruments-Q 800 (New Castle, DE, USA), equipped with tension clamps. One end of the strand was attached to a superior mobile clamp and the other end attached to a lower fixed clamp. Amplitude sweeps were first performed in order to determine the linear viscoelastic range (LVR). Normal storage (E') and loss (E'') moduli as well as strain were recorded as a function of stress, at a constant frequency of 1 Hz and a temperature of 25 °C. The constant strain value to work in the following frequency sweeps was chosen from the firstly determined LVR for each film sample, where a linear relationship existed between strain and stress. Each mechanical spectrum was then obtained at a constant strain value: E' and E'', as well as the loss factor $\tan\delta = E''/E'$, were recorded over at least three decades of increasing angular frequency (ω; rad s^{-1}), after reaching steady state condition for each point. At least, ten replicates of each condition were measured.

Dissipated over stored energies was calculated as indicated by Ferry (1980),

$$\varepsilon_{diss}/\varepsilon_{stored} = 2.\pi.\tan\delta$$

2.4.3. Tensile stress-strain behavior

For quasi-static test in uniaxial condition, a preload force of 10^{-2} N and a constant force ramp rate of 1 N/min were applied to record the stress-strain curves until rupture from film sample strips, using the same DMA and procedure to fix them to the clamps as in the case of dynamic tests. Tests were carried out at 25 °C. The ultimate tensile strength or material resistance at failure was calculated as the ratio between the stress and the strain-at-break (Ferry, 1980). At least, ten to twelve replicates of each condition were measured.

In order to calculate the elastic modulus at large deformations (E_C), stress-strain curves were fitted to Eq. (1):

$$\sigma_T(\varepsilon_T) = E_C.\varepsilon_T.\exp(\varepsilon_T.K) \quad (1)$$

which is adequate for data acquired under constant force ramp rate (Del Nobile, Chillo, Falcone, Laverse, Pati, & Baiano, 2007). Herein, K is a constant considered as a fitting parameter.

Experimental stress-strain curves were analyzed through fitting of them to the model proposed by Kawai, Nitta, and Nishinari (2007), which is a form of the strain energy function based on a power expansion of the free energy (W).

$$W = \boldsymbol{GI} + \boldsymbol{BI}^{m} + \boldsymbol{CI}^{k} \quad (2)$$

with powers $k > m > 1$, and three coefficients $\boldsymbol{G}$, $\boldsymbol{B}$ (strain hardening) and $\boldsymbol{C}$ (strain softening). To accomplish this, experimental curves were plotted as stress *vs* stretch ratio (λ), where λ is the ratio of transient sample dimensions to the original dimensions in the principal axes. By adopting Rivlin formulation, free energy W can be expressed in terms of the strain invariant $\boldsymbol{I}$:

$$I = \frac{1}{2}\left(\lambda_1^2 + \lambda_2^2 + \lambda_3^2 - 3\right) \quad (3)$$

In the strain by simple elongation of an incompressible material, where the volume remains unchanged, the principal extension ratios λ_1, λ_2 and λ_3 are given by (Treloar, 1958):

$$\lambda_1 = \lambda; \quad \lambda_2 = \lambda_3 = \lambda^{-1/2} \quad (4)$$

According to this and taking into account that the only force acting is the tensile force in the direction of the λ-extension, the magnitude of the force per unit of cross-sectional area measured in the unstrained state (the σ-stress) can be expressed as:

$$\sigma = \frac{dW}{d\lambda} = \left[G + mBI^{(m-1)} + kC^{(k-1)}\right]\left(\lambda - \frac{1}{\lambda^2}\right) \quad (5)$$

which predicts that, at low strains (<30% of strain, according to statistical theory; Ferry, 1980), the stress is linearly proportional to the Hookean strain, whereas at higher strains, the behavior becomes non-linear. Eq. (5) is the mathematical expression for fitting the experimental curves of stress *vs* stretch ratio.

Goodness of fit was evaluated by using the coefficient of determination (Kawai et al., 2007) defined by

$$R^2 = 1 - \frac{\sum_i \left(\sigma_i - \sigma_i^{fit}\right)^2}{\sum_i \left(\sigma_i - \overline{\sigma}\right)^2} \quad (6)$$

2.5. Atomic force microscopy (AFM)

This study was performed on film samples stored at the lowest relative humidity of storage (33.3%) in order to avoid the interference of water vapor in the technique as well as under nitrogen atmosphere, for the same purpose. Images were taken by using an atomic force microscope (NanoScope III, Digital Instruments, CA, USA) provided with a silicon-cantilever of 40 N/m-elastic constant operating at 300 kHz of resonance frequency, for imaging at tapping mode. Scan size was set to obtain 5.0×5.0 μm or 1.0×1.0 μm-images. Image analysis was performed through the scanning probe microscopy software WSxM 4.0 Develop 11.3-Package (2007, Nanotec Electronica, Spain) and according to Horcas, Fernandez, Gomez-Rodriguez, and Colchero (2007).

2.6. Statistical analyses of data

Non-linear fitting of experimental results was performed through GraphPad Prism (Version 5.00, 2007, USA) and Solver function of the Microsoft Excel Program (2002, Microsoft Corp., USA).

Statistical analyses of results were performed through ANOVA with α:0.05, followed by pair wise multiple comparisons evaluated by Tukey's significant difference test (Sokal & Rohlf, 1995). The Statgraphic software (version 5.1, 1994–2001, Rockville, MD, USA) was used.

3. Results and discussion

3.1. Dynamic normal test

Experimental investigation under normal oscillatory conditions in the linear viscoelastic regime was performed for rheological characterization of the polysaccharide films herein studied, in order to achieve structural discrimination. Constant strains of 0.03% for C-films stored at 75.2%-RH or 0.1%, for the others, were used to work at linear condition in the frequency sweeps, according to results obtained in amplitude sweeps that were performed at 1 Hz of constant frequency and 25 °C.

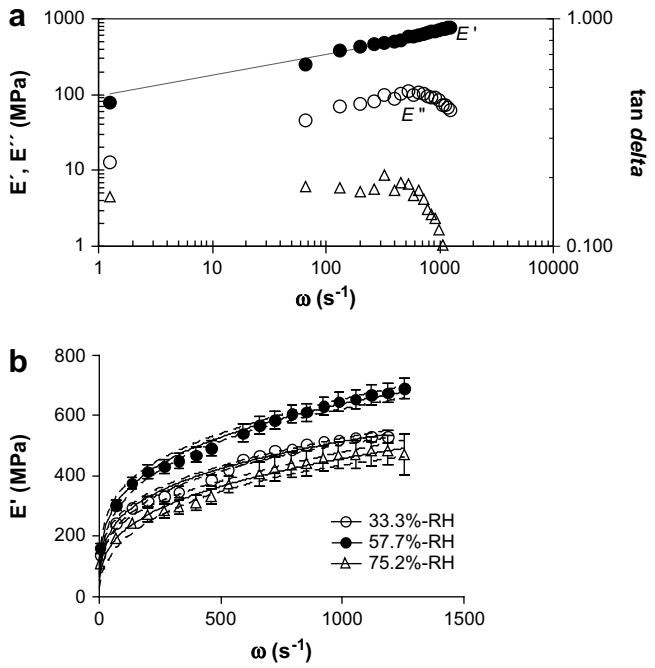

Fig. 1. (a) Dynamic mechanical spectrum of D-film system determined at 25 °C in linear conditions, showing the normal storage (E') and loss (E'') moduli, as well as tangent of phase angle (tan δ), and fitting of experimental data (points) to the exponential equation (continuous lines). The latter is better observed in panel (b), where 95%-confidence bands are shown against linear axes, for the different relative humidity (RH) levels used for film storage, at 25 °C.

The mechanical spectra of films can be observed in Fig. 1a, for system D, as an example; spectra were taken along three decades of frequency between 0.2 and 200 Hz ($w = 1.256$ and 1256 s^{-1}). They showed the characteristic profiles of real biopolymer gel systems, herein characterized by only a slight increase of the storage normal modulus E' with the frequency in the 1.256–1256 s^{-1}-ω-range studied (Doublier, Launay, & Cuvelier, 1992). At the same time, loss normal modulus E'' was, in general, parallel and one log cycle lower than E' along this frequency range, which corresponded to the mechanical spectra of a viscoelastic solid-like material. The slight frequency dependence of moduli seemed to change with the polymer system, therefore E'-experimental data of each spectra was adjusted with $E' \propto \omega^n$ as reported in the literature for other polysaccharide systems (Ross-Murphy, 1994; Lapasin & Pricl, 1995), in order to compare the dependence observed. Storage modulus showed good agreement with the exponential model proposed (Fig. 1b) for all film systems in the frequency range assayed. It can be observed (Table 2) that D-mix films showed the highest frequency dependence (n) of E' at the three relative humidities of storage, showing the same n-value at 33.3 and 57.7%-RH. Gellan and C-mix films showed similar frequency dependence (n) at each RH studied, which was not affected by RH. The same can be observed for E_0' with the exception of C-film stored at 75.2%-RH which showed its lowest value of E_0' (92 MPa). With the exception of system A, films stored at 33.3 and 57.7% presented slightly higher storage moduli ($\approx$700 MPa at $\omega = 1000$ rad s^{-1}) than those showed after storage at 75.2%-RH ($\approx$550 MPa at $\omega = 1000$ rad s^{-1}), though in the same order of magnitude.

The exponential $E'' \propto \omega^n$ was not adequate to explain the frequency dependence of loss moduli for films stored at the two lowest RH, since at a given ω-value (722 s^{-1}), E'' began to decrease with frequency increase (shorter time scale), whereas E' was still increasing (Fig. 1a). This fact was stressed by the damping factor ($\tan\delta = E''/E'$) when plotted against frequency for all film systems (Fig. 2), where tan δ was constant ($\approx$0.1500) up to around 722 s^{-1}. After this frequency, tan δ continuously decreased to 0.0700 or 0.0400 for films stored at 33.3 and 57.7%-RH, respectively. These events manifest the change in the ratio of dissipated over stored energies ($\varepsilon_{diss}/\varepsilon_{stored}$), which showed a decrease from 0.98 to 0.20 in film systems stored at 57.7%-RH while those at 33.3% showed a decrease from 0.94 to 0.62. On the other hand, films stored at 75.2% presented a constant tan δ along the studied frequency range, which was $\approx$0.1600 for D- and Ca-gellan films and $\approx$0.1300 for C- and gellan films. All systems herein assayed were basically amorphous rubbers at 25 °C having Tg values between −85.21 and −113.9 °C as determined by DSC (León et al., 2008). Film casting and further storage at controlled relative humidity, resulted in the development of an amorphous matrix, which is a non-equilibrium state with time-dependent properties (Pittia & Sacchetti, 2008). Polysaccharides constitute transient networks since these polymers interact essentially through hydrogen bonds between them, as well as with the remaining water and glycerol plasticizing molecules. Cross-links between these food polymers originated from physical interactions, often hydrogen bonds, but electrostatic, van der Waals and hydrophobic interaction forces, may also be important as occur in some gels. Ion bridging type-interactions, involving the presence of divalent cations, mainly Ca^{2+}, are very important in many cases like in gellan polymer (Doublier, Launey, & Cuvelier, 1992; Ross-Murphy, 1994; Tang, Lelievre, Tung, & Zeng, 1994; Nickerson, Paulson, & Speers, 2003; Nickerson & Paulson, 2004). As it was indicated by Gunning, Kirby, Ridout, Brownsey, and Morris (1996), gellan particularly constitutes a fibrous gel network in the presence of gel-promoting cations, where the entire structure is effectively a junction zone. They suggested that the permanency of the gel network arises from ion binding between

Table 2
Parameters[a] obtained after fitting of experimental normal storage modulus (E′) data to the exponential equation $E' \propto \omega^n$, at 25 °C.

Relative humidity (%) of film storage		Gellan films (A)	Ca-gellan films (B)	C-films	D-films	F[b]
33.3%	Moisture content (g/100 g dm)	21.9 ± 0.4	24.0 ± 0.3	25.9 ± 0.6	28.4 ± 0.4	
	E_0'	188 ± 41	139 ± 19	218 ± 27	76 ± 6	138.7
	n	0.20 ± 0.03	0.21 ± 0.02	0.19 ± 0.02	0.28 ± 0.01	
57.7%	Moisture content (g/100 g dm)	30.1 ± 0.5	29.1 ± 0.5	28.8 ± 0.3	31.6 ± 0.6	
	E_0'	199 ± 32	194 ± 30	190 ± 29	97 ± 10	45.22
	n	0.21 ± 0.02	0.17 ± 0.02	0.22 ± 0.02	0.27 ± 0.01	
75.2%	Moisture content (g/100 g dm)	39.6 ± 0.3	41.9 ± 0.4	33.6 ± 0.3	39.9 ± 0.6	
	E_0'	203 ± 36	71 ± 18	92 ± 10	49 ± 9	76.93
	n	0.18 ± 0.03	0.30 ± 0.03	0.21 ± 0.02	0.32 ± 0.03	

[a] Standard errors are shown ($\alpha = 0.05$).
[b] F statistical parameter for comparison between fitted curves, which rejected the null hypothesis ($P < 0.0001$) of one curve for all data set. Hence, there is a different curve for each treatment.

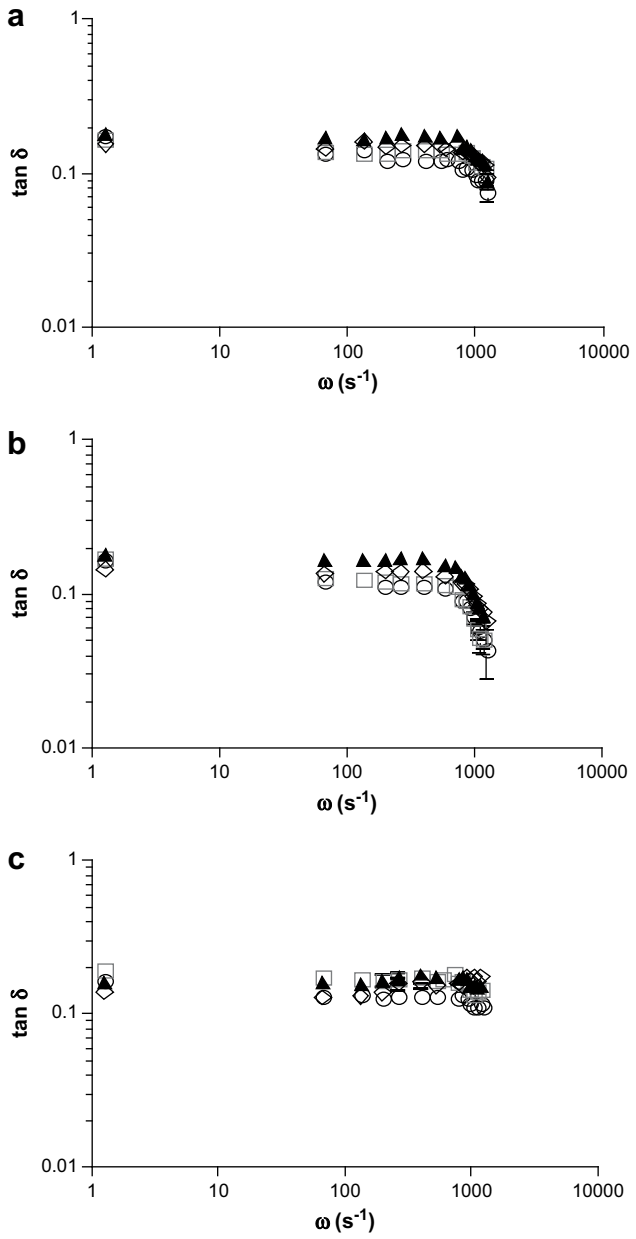

Fig. 2. Tangent of the phase angle (tan δ) determined through the mechanical spectra for A- (○), B- (□), C- (◇) and D-films (▲) stored at 25 °C, and 33.3% (a), 57.7% (b) or 75.2% (**c**) relative humidity.

gellan helices stacked side by side within the fibers, where cation binding is considered to cause the observed hysteresis in melting and setting of gellan gels. In the case of the acid-set gellan gels, like the system A herein studied, Gunning et al. (1996) informed that hysteresis was enough to make the gel thermally irreversible.

Only film systems stored at 33.3 and 57.7%-RH showed tan δ -diminishing from 722 to 1260 s^{-1}. Such film systems behaved as solids because the time scale of the observation was shorter than the lifetime of the physical cross-links (Doublier et al., 1992). As a consequence, the behavior observed for tan δ might be attributed to the fact that the period of oscillation was long compared to the relaxation time of some physical cross-links of the network strands (Grassi, Lapasin, & Pricl, 1996). Penetration of water molecules constrained pre-existing mobile network regions or could lead to association of polymer chains which is facilitated by enhanced macromolecular mobility in the rubbery state (Pittia & Sacchetti, 2008). This effect was not significant in films stored at 75.2%-RH (Fig. 2), leading to think about polymer interactions, at this RH, characterized by longer relaxation times with respect to the time scales of the performed experiment. The latter stage may be associated with a polymer network which was definitively plasticized by enough water to accomplish this, interacting in presence of glycerol. Consequently, there is evidence of a shorter relaxation time in the 33.3–57.7%-films which may influence the small deformation (linear range) measurements. The mentioned shorter relaxation times may involve different interactions (i.e.: polymer–polymer, polymer–water).

3.2. NMR

The spin–lattice relaxation decay was found to be a single exponential (T_1) for all films studied. The spin–spin relaxation showed two water populations, T_{2a} and T_{2b} (León et al., 2008)

The relationship between T_1, T_2 and solid fraction can be observed in Fig. 3. Addition of water to the systems resulted in a decrease in the T_1. This indicates that water provided a relaxation path for the macromolecule protons. Spin–spin relaxation increased in rate (T_2^{-1}) with increasing solid concentration. The increase of T_1 with solid concentration higher than 0.770 is expected for solid samples in the rigid–lattice regime. In this regime, spin–lattice relaxation is slow, the lifetime of the individual spin states is short because the excitation passes via mutual spin-flips to other spins. Therefore, T_1 is long but T_2 is short (Kou et al., 2000).

As can be also observed in Fig. 3, the spin–lattice relaxation rate of ^{1}H-water (T_1^{-1}) was lower when acylated– deacylated gellan mixtures (C- and D-systems) were used.

3.3. Stress-strain assay

Fig. 4 shows the tensile stress (σ)-strain (ε) behavior of the films acquired at constant force ramp rate of 1 N/min until rupture. Percents of strain-at-break were low, between 2.7 (A- and B-systems) and 9.5% (C- and D-films), (Fig. 5a), which is showing a behavior typical of hard and brittle polymer networks. These stress-strain profiles are the result of reduced moisture content (Table 2), which promoted intermolecular forces and strong ionic interaction (Li, Dickinson, & Chinachoti, 1998; Yang & Paulson, 2000; Vittadini, Dickinson, & Chinachoti, 2001).

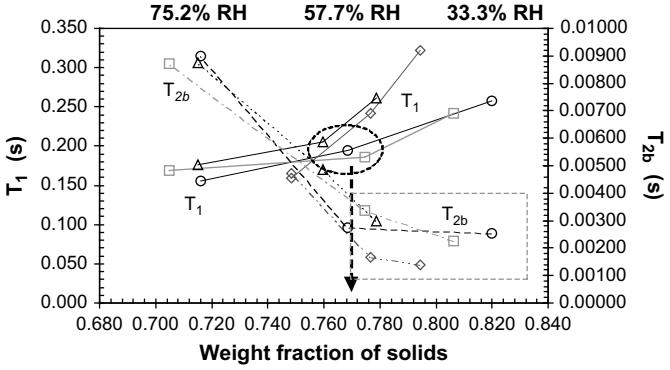

Fig. 3. ^{1}H-NMR T_1 (spin–lattice) and T_2 (spin–spin) relaxation times determined for A- (○), B- (□), C- (◇) and D-film (△) systems stored at 25 °C and 33.3, 57.7 or 75.2% of relative humidity (RH), plotted as a function of sample weight fraction of solids. Standard deviations ($n = 4$) are in the order of the symbol size.

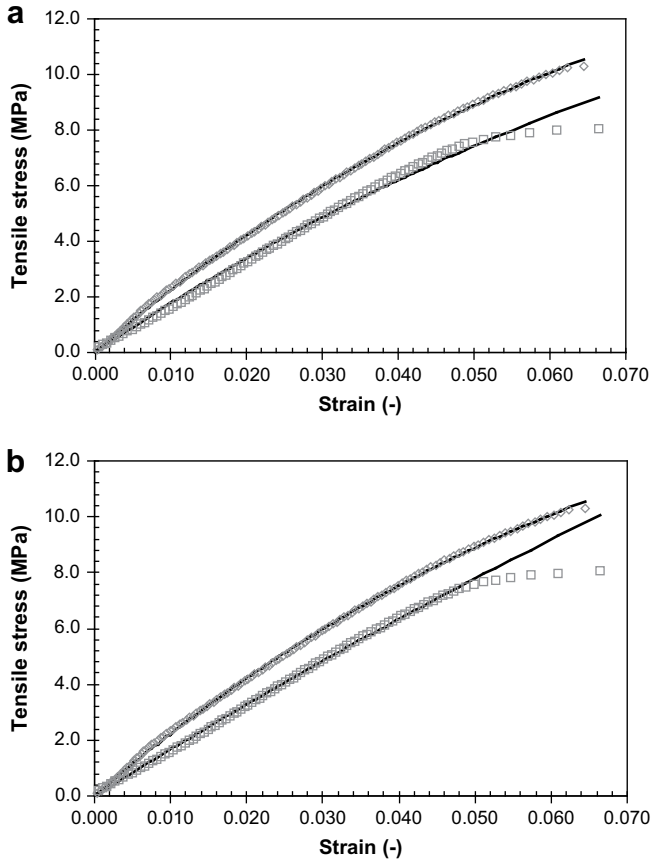

Fig. 4. Curves of tensile stress *vs* strain determined until failure from B- (□) and C-film (◇) systems, which were previously stored at 33.3 and 57.7%, respectively. Experimental data were obtained at 25 °C and under a constant force ramp rate of 1 N/min. Continuous lines are indicating data fitting to Eq. (1), considering all data until rupture (a), or no taking into account the last 5 points of B-system curve (b).

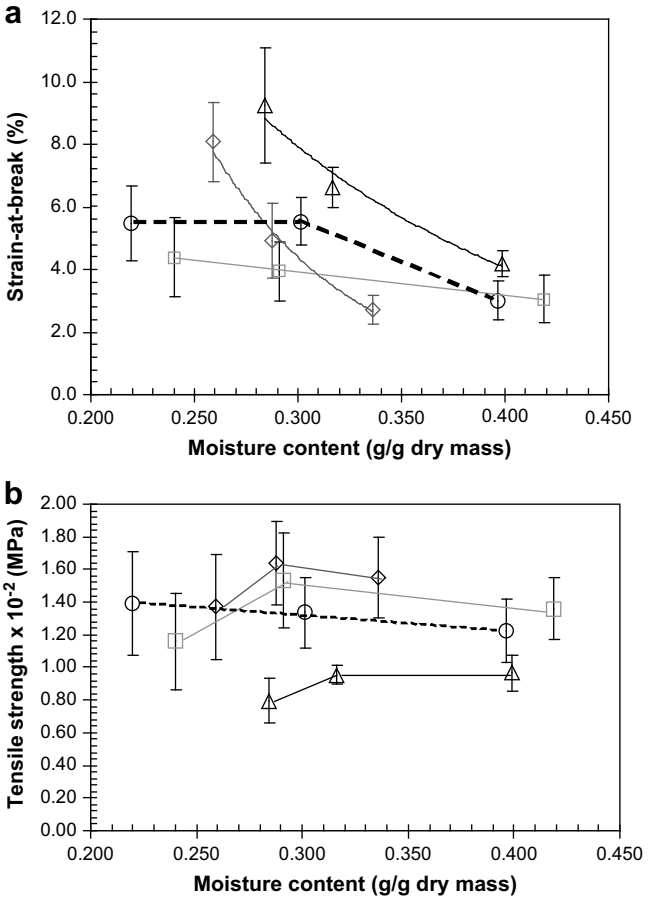

Fig. 5. Strain-at-break (a), and tensile strength or material resistance at break (b) plotted as a function of moisture content of A- (○), B- (□), C- (◇) or D-films (△) stored at 25 °C, and 33.3, 57.7 or 75.2% of relative humidity.

In this paper it was observed that strain-at-break was significantly affected by moisture content. As can be observed in Fig. 5a, when acylated–deacylated gellan mixtures (C- and D-systems) were used for film making, strain-at-break increased with decrease in moisture content, which is coincident with an increase in T_{2b}^{-1}. As well, higher strain values were found when a higher proportion of glycerol (D-films) was used. On the other hand, gellan based (A- and B-) films only showed a decrease of the strain-at-break at the highest moisture contents (Fig. 5a), with some non-significantly lower strain-at-break when calcium was added (B-films). Similar trend was shown by the stress-at-break. As a result of the ratio between the stress and strain-at-break, only some non-significant increase was observed in tensile strength with the moisture content into each film system. C-films showed high values of strain-at-break and the highest tensile strength (Fig. 5b), while D-films showed the lowest tensile strength. As it was suggested from the dynamic results obtained, the increase in moisture content with the relative humidity of storage might allow association of polymer chains, which is facilitated by enhanced macromolecular mobility in the rubbery state (Pittia & Sacchetti, 2008). Penetration of water molecules into the polymeric networks produced their constraint, evidenced by the inverse relationship between strain-at-break and moisture content (Fig. 5a). Gellan based films were more brittle than acylated–deacylated gellan films, since when equilibrated at 33.3%-RH they showed the lowest strain-at-break; acylated–deacylated gellan mixtures, probably had a faster relaxation of the macromolecules into the strands as a consequence of lower polymer interaction, which permits faster accommodation under the stress applied, determining higher strain-at-break. It can be concluded that the different microstructures of each film network (A-, B-, C- or D-system) involving polymer–polymer, water–polymer, water–polymer–glycerol interactions, affected results obtained.

There is a basic difference between rupture above the Tg, where the polymer chain backbones have an opportunity to change their configuration before the sample fails, and below Tg, where the backbone configurations are essentially immobilized within the period of the experiment. Polymers not chemically cross-linked and at temperatures far above Tg, probably rupture with bond breakage unless the deformation is sufficiently slow, as in the present assay, to permit escape of the molecules from their topological restraints; the process of rupture depends enormously on the rate of deformation, according to Ferry (1980).

Elastic modulus at large deformations (E_C) was calculated by fitting Eq. (1), to data acquired at constant force ramp with the object of comparison of different materials. The relationship between stress and strain, which corresponded to the Young's modulus, was here affected (1) by an exponential term which acts as a damping factor. As it can be observed in Fig. 4a, for system B, Eq. (1) was not adequate to completely explain the stress-strain experimental curve recorded from gellan based (A- and B-) films at deformations higher than 5%. Consequently, it was necessary to delete the points immediately before rupture in the systems mentioned, in order to obtain a better fitting of the experimental

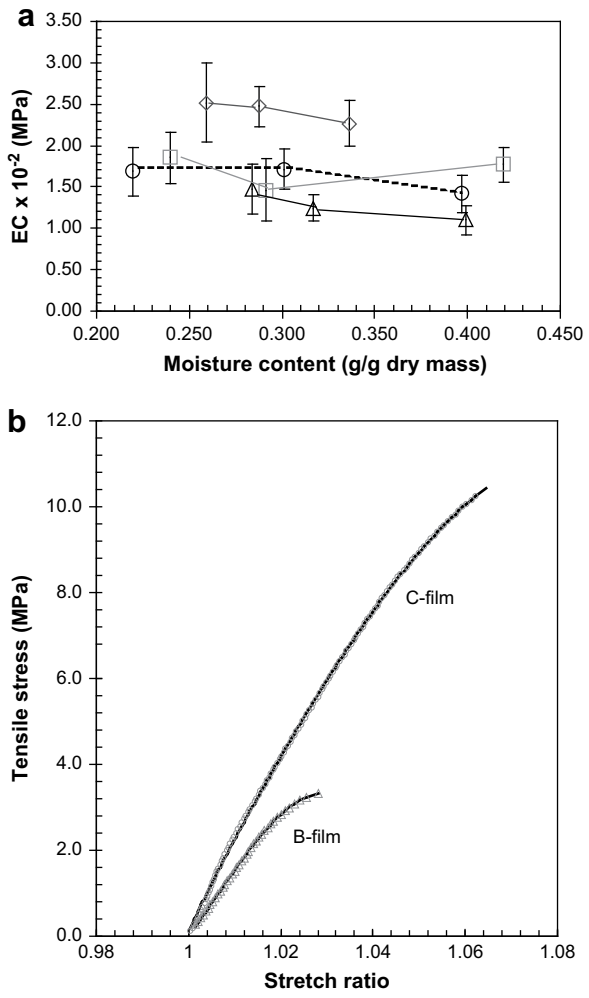

Fig. 6. (a) Elastic modulus at large deformation scale (E_C parameter) determined from adjustment to Eq. (1) of experimental data reported in Fig. 4. It was plotted as a function of moisture content of A- (○), B- (□), C- (◇) or D-films (△) stored at 25 °C, and 33.3, 57.7 or 75.2% of relative humidity. (b) Experimental curves (points) of tensile stress like those of Fig. 4, but herein plotted against stretch ratio; continuous lines indicate the curves drawn through the fitting of Eq. (2), which is based on a power expansion of the free energy (W).

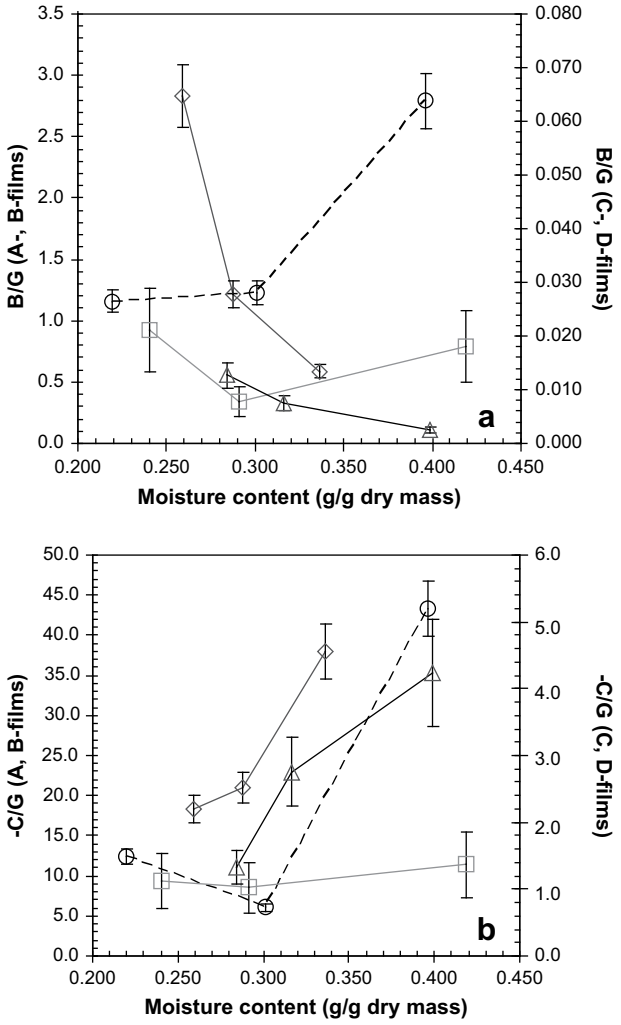

Fig. 7. (a) Hardening degree (**B/G**), as well as (b) softening degree (**C/G**) plotted as a function of moisture content of A- (○), B- (□), C- (◇) or D-films (△) stored at 25 °C and 33.3, 57.7 or 75.2% of relative humidity. Parameters (**G, B, C**) were obtained by adjustment of curves like those shown in Fig. 6b, to Eq. (2).

points at initial and intermediate deformations (Fig. 4b). As it can be observed on Fig. 6a, E_C was almost non -significantly dependent on moisture content for each film system studied.

Edible films based on acylated–deacylated gellan mixtures showed the highest E_C when the lowest proportion of glycerol (C-films) was used as plasticizer (Fig. 6a), whereas this network presented the lowest elastic modulus under large deformations when glycerol was used in the same proportion (D-system) used for gellan based films (A- and B-). As it could be concluded from the comparison of strain-at-break, acylated–deacylated gellan mixtures produced films with a less rigid polymeric network, fact that allowed to depress glycerol concentration without impairing mechanical properties. Glycerol content depression might contribute to L-(+)-ascorbic acid retention (León & Rojas, 2007).

With the aim of better exploring the mechanism of elasticity by which the gellan fibers manifest themselves in the film networks, experimental stress-strain curves were analyzed through the fitting of them to the model proposed by Kawai et al. (2007) which is a form of strain energy function (Eq. (2)); the model was adapted to simple elongation-tensile condition used in this research. The theory of non-linear viscoelasticity was considered in this model. It is of interest because the behavior of viscoelastic solids at the limits of the time and frequency range is elastic. At short times or at long times and low frequencies, memory effects become negligible and the material can be considered elastic (Anniek de Bever, 1992).

As an example, curves of stress *vs* stretch ratio (λ) until failure for systems A and D, are shown in Fig. 6b. It can be observed that experimental data are completely described ($R^2 \approx 0.9998$–0.9999; Eq. (6)) by this five-parameters-Eq. (2), which is based on a power expansion of the free energy (W). As a characteristic property of power expansions, each term becomes effective in different regions. The stress *vs* stretch ratio (tensile strain invariant $I \approx 0$), showed that at very small deformation the first term is dominant. The second term, becomes appreciable when tensile deformation is increased and, after that, the third term becomes significant because of $k > m > 1$. As determined by Kawai et al. (2007) for compression of gellan gels, our films showed hardening at intermediate strains or stretch ratios and softening in large deformations before rupture in tensile conditions. It was determined that gellan based films (A- and B-systems) presented a higher power ($m = 3.0$) in the second term, indicating a relative more important weight of the invariant factor to the hardening phase of the curve in

comparison with that ($m = 1.5$) of films elaborated with a mixture of acylated–deacylated gellan polymers. Higher rigidity characterized gellan based films (A- and B-networks) at intermediate deformations, which can also lead to higher strain-softening degree till rupture (Kawai et al., 2007). This fact may be associated to enhanced polymer interactions in deacylated gellan polymers. It has been reported that entanglement effects result in strain-hardening (Rubinstein & Panyukov, 1997). Conversely, hindering occurs in the case of acylated gellan polymers in C- and D-networks due to side acyl groups determining lower "***B***" and "***C***" parameters.

Fig. 7a shows the moisture content dependence of the fitting parameter ***B***, which describes strain hardening divided by ***G***. Although different *m*-power in the invariant factor, it could be in part compared the relative importance of B parameters in the second term. In this sense, higher ***B***/***G*** values can be observed for A and B-films with respect to those presented by acylated–deacylated gellan (C- and D-) systems; a decrease of ***B***/***G*** with moisture content decrease for A- and B-systems and an increase of ***B***/***G*** with moisture content decrease for C- and D-systems. Probably, at high moisture contents, the amorphous rubbery systems A and B had gained enough mobility to permit additional macromolecular association.

All film formulations needed the same power ($k = 4.5$) for the softening phase immediately before rupture and, hence, showed the same contribution of the invariant factor to strain at large deformations near the rupture point. Fig. 7b shows the moisture content dependence of the fitting parameter ***C***, which describes, strain softening divided by ***G***. Considerable higher ***C***/***G*** values were observed for gellan based (A- and B-) films. The highest relative softening degree was showed by A-system stored at 75.2%-RH and the lowest by D-films equilibrated at 33.3%-RH. A significant increase in the degree of softening with moisture content was shown by A-, C- and D- films. B- films were not affected by moisture content, probably due to Ca^{2+} effect in the network. The low softening degree observed for C- and D-systems may be also ascribed to spatial hindering due to the presence of acyl groups.

3.4. Atomic force microscopy

Fig. 8 shows AFM images for the film systems herein formulated, where homogeneous and continuous branched fibrous networks can be observed as their microstructure in the 1.0 μm × 1.0 μm scale; images observed are similar to those earlier determined by Gunning and collaborators (1996) for gellan gels. Above the critical or threshold concentration for gelation, gel precursors are themselves assembled into a single fibrous network in the presence of gel-promoting cations (e.g., calcium). Side-by-side association of a few gellan helices is compatible with the high transparency of the gels, as it was observed in gellan based films (A- and B- systems). On the other hand, presence of acylated gellan polymer, in the formulation, produced film networks with some opacity (C- and D-systems).

The images contain regions which appear dark and others which are bright or flared. This effect arises due to the curvature or roughness of the film surfaces. Gellan based films (Figs. 8a,b) show thick fibers which seemed to be in bunches, and almost completely fill the image. Topographical analyses rendered fibers ranging from, at least 39.202 to 57.295 nm-thick. Arrows in Fig. 8a indicate each (23.534, 24.326 nm) of two distinguishable fibers of a 75.859 nm-

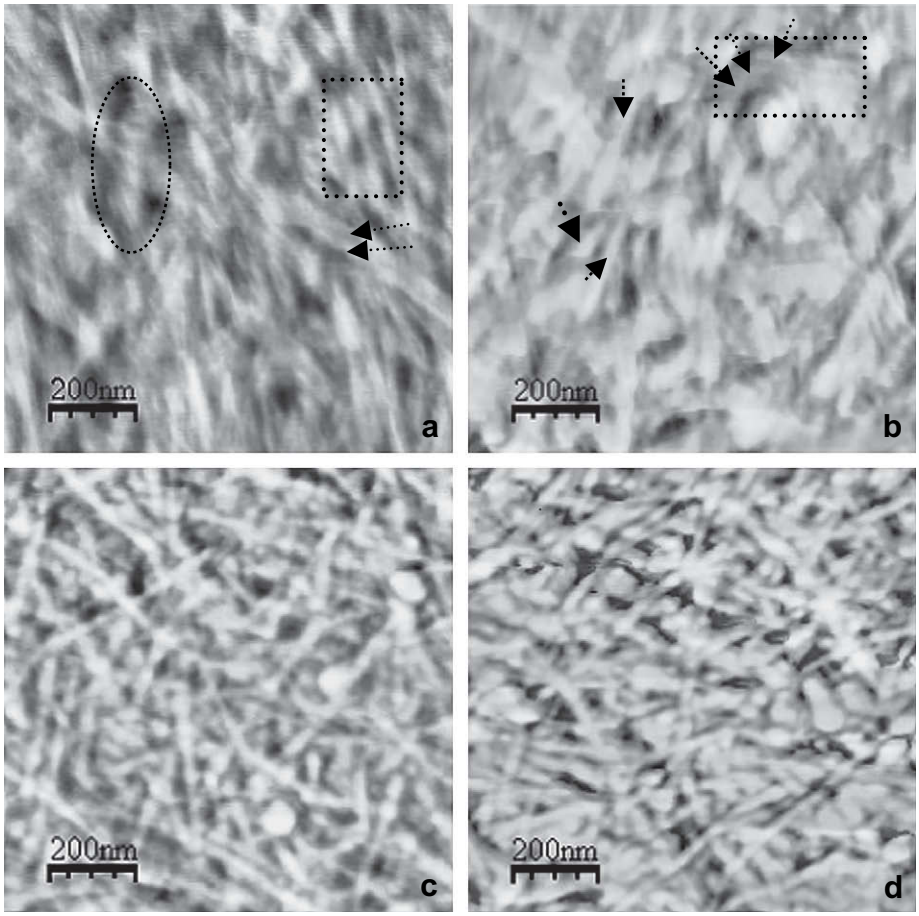

Fig. 8. Atomic force microscopy images taken with a scan size of 1.0 × 1.0 μm from (a) gellan (A-), (b) Ca-gellan (B-), as well as from acylated–deacylated gellan mix (c) D- and (d) C-films.

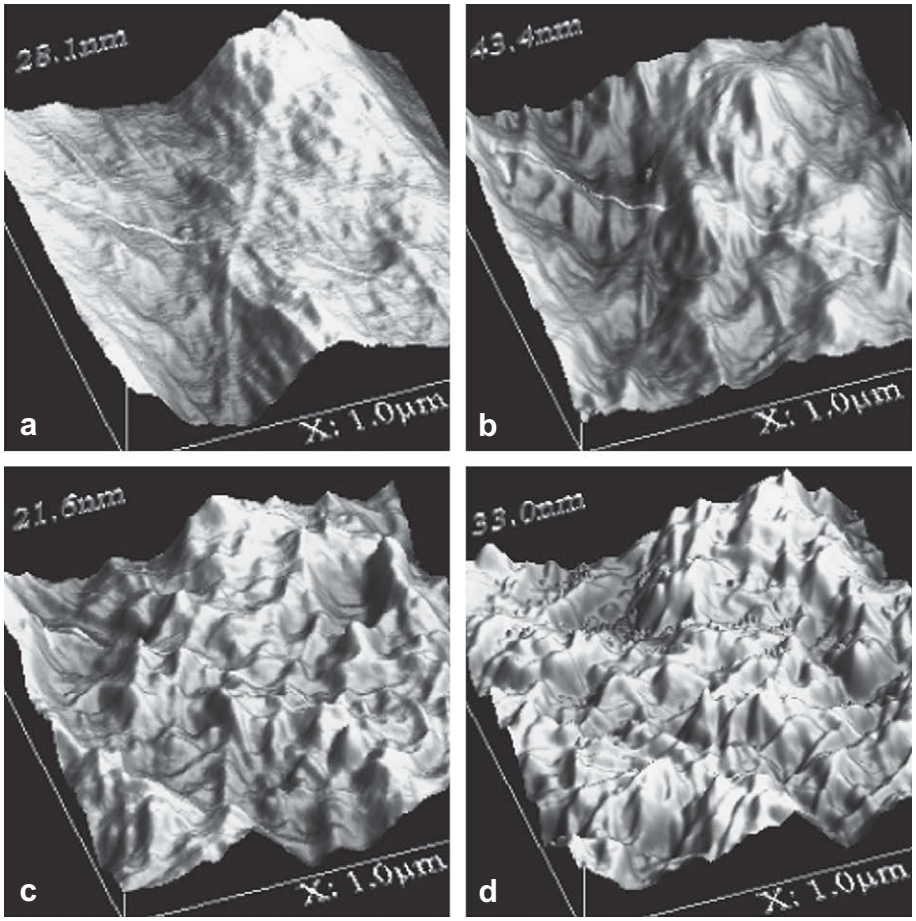

Fig. 9. Topographical images of the in phase scans showed in Fig. 8 (1.0 × 1.0 μm) for (a) gellan (A-), (b) Ca-gellan (B-), as well as for acylated–deacylated gellan mix systems (c) D- and (d) C-films, which are plotted in three dimensions.

width-bunch, while three fibers of 26.775, 27.698 and 28.622 nm (square, Fig. 8a) seem to take part of a complex pattern where individuals are woven together. The latter can also be seen in the ellipsoid where three parallel fibers are surrounding a vertical bunch. Fig. 8b, where the network can be considered as a system mediated by ionic (Ca^{2+}) interactions (Nickerson et al., 2003), mainly showed thick bunches, being the constituent fibers not easily distinguishable.

Acylated–deacylated gellan based films (C- and D-systems) produced networks with more clearly defined fibers, which cross-over to each other more frequently and in different directions. As there are weft and warp strands, more knots are observed in these nets. Their topography revealed 32.251–16.027 nm-thick fibers and strands of 110–160 nm in length. This pattern of frame (knots and strands) can be better observed when micrographs of topography are plotted in three dimensions: Figs. 9c,d show a sharp relief. Conversely, gellan A-film presented a flat surface (Fig. 9a), whilst gellan (deacylated) polymer with extra calcium addition (B-films) showed some sharper relief (Fig. 9b), which can be associated to the thicker bunches determined from the topography of Fig. 8b. Hence, it can be concluded that either the presence of more extended junction zones along the entire B-film network (Fig. 9b) in a system mediated by ionic (Ca^{2+}) interactions, or presence of side chains in the gellan polymer (Figs. 9c,d) determined the loss of the flat topography which characterized deacylated gellan film (Fig. 9a). On the other hand, association and lateral aggregation of gellan fibers to form thick bundles seemed to be the way for film network development in A- and B-systems. Conversely, presence of acylated gellan macromolecules in C- and D-formulations hindered lateral aggregation to form bunches, leading to thinner fibers organized like wefts and warps for the film network.

Dehydration of each kind of polymer gel during casting of films gave origin to fibrous networks (Fig. 8), which evidence the high density of hydrogen bonds, as well as the ion binding interhelical association between polymers (mainly in the B-system , Fig. 8b) present in fibers; these bonds are implicated in network permanency and are supporting normal stress along mechanical tests.

4. Conclusions

Films developed for supporting L-(+)-ascorbic acid were rheologically evaluated. Under the conditions stated, the studied systems showed the characteristic profiles of real biopolymer gel systems.

There was evidence for shorter relaxation times in relation to the time scale of the experiment, for films stored at 33.3–57.7%-RH, which may influence small deformation measurements. At 33.3 and 57.7%-RH, films showed tan δ diminishing for ω higher than 722 s^{-1}. Probably, the period of experimental oscillation was long compared to the relaxation time of some physical cross-links of the macromolecular network at those conditions. According to NMR studies, at 33.3 and 57.7% of moisture storage, films studied seemed to be in rigid–lattice regime. Probably, this regime determined the behavior observed for systems stored at these relative humidities.

The use of a mixture of acylated–deacylated gellan polymer determined a decrease in the elastic modulus at large deformations

(E_C), while the diminishing of glycerol in this system produced the highest film-E_C for each relative humidity tested.

By analyses of the parameters derived from fitting stress-strain curves to a form of the strain energy function in tensile condition, hardening effect was observed at intermediate strains and softening at extreme deformations till rupture. Hardening degree may be related to enhanced polymer interactions as expected from gellan based films (A- and B-systems), and its increase with the water content may be a result of macromolecular association and favored lateral aggregation. Higher rigidity may also lead to the higher strain-softening degree till rupture observed for these films. Conversely, spatial hindering in the film network as a consequence of acylated gellan presence produced a smaller hardening degree due to worsened polymer interactions, effect which was also dependent on the moisture content. The low softening degree observed for acylated–deacylated systems may also be attributed to the spatial hindering along aggregation.

Atomic force microscopy bidimensional images showed different morphological characteristics for A,B- and C,D-systems. A- and B-systems developed the network through association and lateral aggregation of fibers giving origin to thick bundles. Conversely, presence of acylated gellan macromolecules in C- and D-films hindered lateral aggregation to form bunches, leading to thinner fibers organized like wefts and warps in the network. Three dimensional images showed that presence of more extended junction zones mediated by Ca^{2+} or presence of side chains due to acylated gellan, determined the loss of the flat topography that characterized deacylated gellan films.

In physically cross-linked systems, like edible films herein studied, the density and lifetime of the junction zones govern the mechanical properties of the network and its responses to applied stress or strain. At the same time, rheological properties are useful in developing structure–function relationships. In this context, it was important to accomplish mechanical characterization of edible films due to its influence on product performance and consumer acceptance of foods which were provided by the antioxidant protection of the active edible films herein developed.

Acknowledgements

We acknowledge the financial support from Universidad de Buenos Aires (UBA), Agencia Nacional de Promoción Científica y Tecnológica de la República Argentina (ANPCyT), National Research Council of Argentina (CONICET) and SECyT-MAE. We are also grateful to Lic. Mónica Maritano (Biotec, Argentina) and Lic. Graciela Guananja (CP Kelco) for their attention with respect to our needs for CP Kelco food gums which were provided without costs by the Company; to Dr. Gustavo A. Monti, Lic. Belén Franzoni and Lic. Yamila Garro Linck of the LANAIS (Laboratorio Nacional de Investigación y Servicios) of Nuclear Magnetic Resonance (NMR) of solid materials, Facultad de Matemática, Astronomía y Física (FaMAF), Universidad Nacional de Córdoba, Argentina, for their help with NMR analysis, as well as to Lic. Silvio Ludueña and Dr. Lía Pietrasanta, for their assistance to take the atomic force microscopy images at the "Centro de Microscopías Avanzadas, CMA", Department of Physics, Facultad de Ciencias Exactas y Naturales, Universidad de Buenos Aires, Argentina.

References

Anniek de Bever, 1992. Dynamic behavior of rubber and rubber-like materials. WFW-report 92.006, pp. 1–70, *at*: http://alexandria.tue.nl/repository/books/628061.pdf.

Bengoechea, C., Arrachid, A., Guerrero, A., Hill, S. E., & Mitchell, J. R. (2007). Relationship between the glass transition temperature and the melt flow behavior for gluten, casein and soya. *Journal of Cereal Science, 45*(3), 275–284.

Chandrasekaran, R., Puigjaner, L. C., Joyce, K. L., & Arnott, S. (1988). Cation interactions in gellan: an X-ray study of the potassium salt. *Carbohydrate Research, 181*, 23–40.

Del Nobile, M. A., Chillo, S., Mentana, A., & Baiano, A. (2007). Use of the generalized Maxwell model for describing the stress relaxation behavior of solid-like foods. *Journal of Food Engineering, 78*, 978–983.

Del Nobile, M. A., Chillo, S., Falcone, P. M., Laverse, J., Pati, S., & Baiano, A. (2007). Textural changes of Canestrello Pugliese cheese measured during storage. *Journal of Food Engineering, 83*(4), 621–628.

Doublier, J. L., Launay, B., & Cuvelier, G. (1992). Viscoelastic properties of food gels. In M. A. Rao, & J. F. Steffe (Eds.), *Viscoelastic properties of foods* (pp. 371–432). London and New York: Elsevier Applied Science, (Chapter 14).

Famá, L., Rojas, A. M., Goyanes, S., & Gerschenson, L. N. (2005). Mechanical properties of tapioca-starch edible films containing sorbates. *Lebensmittel Wissenschaft und Technologie (LWT), 38*, 631–639.

Ferry, J. D. (1980). *Viscoelastic properties of polymers* (2nd ed.). New York: John Wiley & Sons, USA.

Grassi, M., Lapasin, R., & Pricl, S. (1996). A study of the rheological behavior of scleroglucan weak gel systems. *Carbohydrate Polymers, 29*, 169–181.

Gunning, A. P., Kirby, A. R., Ridout, M. J., Brownsey, G. J., & Morris, V. J. (1996). Investigation of gellan networks and gels by atomic force microscopy. *Macromolecules, 29*, 6791–6796.

Hamcerencu, M., Desbrieres, J., Khoukh, A., Popa, A., & Riess, G. (2008). Synthesis and characterization of new unsaturated esters of Gellan Gum. *Carbohydrate Polymers, 71*, 92–100.

Horcas, I., Fernandez, R., Gomez-Rodriguez, J. M., & Colchero, J. (2007). WSXM: a software for scanning probe microscopy and a tool for nanotechnology. *Review of Scientific Instruments, 78*, 013705.

Kawai, S., Nitta, Y., & Nishinari, K. (2007). Large deformation analysis of gellan gels. *Journal of Applied Physics, 102*(4). 043507 (1–9).

Kou, Y., Dickinson, L. C., & Chinachoti, P. (2000). Mobility characterization of waxy corn starch using wide-line ^{1}H nuclear magnetic resonance. *Journal of Agricultural and Food Chemistry, 48*(11), 5489–5495.

Kristo, E., Biliaderis, C. G., & Zampraka, A. (2007). Water vapour barrier and tensile properties of composite caseinate-pullulan films: biopolymer composition effects and impact of beeswax lamination. *Food Chemistry, 101*, 753–764.

Lai, H.-M., & Padua, G. W. (1997). Properties and microstructure of plasticized Zein films. *Cereal Chemistry, 74*(6), 771–775.

Lapasin, R., & Pricl, S. (1995). Rheology of industrial polysaccharides. Theory and applications. Published by Blackie Academic and Professional, an imprint of Chapman & Hall, Wester Cleddens Road, Bishopbriggs, Glasgow G64 2NZ, UK.

León, P. G., & Rojas, A. M. (2007). Gellan gum films as carriers of L-(+)-ascorbic acid. *Food Research International, 40*, 565–575.

León, P. G., Lammana, M. E., Gerschenson, L. N., & Rojas, A. M. (2008). Influence of composition of edible films based on gellan polymers on L-(+)-ascorbic acid stability. *Food Research International, 41*(6), 667–675.

Li, S., Dickinson, L. C., & Chinachoti, P. (1998). Mobility of unfreezable and freezable water in waxy corn starch by 2H and 1H NMR. *Journal of Agricultural and Food Chemistry, 46*, 62–71.

Mali, S., Grossmann, M. V., García, M. A., Martino, M., & Zaritzky, N. (2005). Mechanical and thermal properties of yam starch films. *Food Chemistry, 101*, 753–764.

Miková, K. (2001). The regulation of antioxidants in food. In J. Pokorny, N. Yanishlieva, & M. Gordon (Eds.), *Antioxidants in foods. Practical applications*. Cambridge, England: CRC Press. Woodhead Publishing Limited. (Chapter 11).

Nickerson, M. T., Paulson, A. T., & Speers, R. A. (2003). Rheological properties of gellan solutions: effect of calcium ions and temperature on pre-gel formation. *Food Hydrocolloids, 17*(5), 577–583.

Nickerson, M. T., & Paulson, A. T. (2004). Rheological properties of gellan, κ-carrageenan and alginate polysaccharides: effect of potassium and calcium ions on macrostructure assemblages. *Carbohydrate Polymers, 58*(1), 15–24.

Pittia, P., & Sacchetti, G. (2008). Antiplasticization effect of water in amorphous foods. A review. *Food Chemistry, 106*, 1417–1427.

Ross-Murphy, SB (1994). In: S.B. Ross-Murphy (Ed.), Physical techniques for the study of food biopolymers. Glasgow: Blackie Academic & Professional (Chapter 7).

Rubinstein, M., & Panyukov, S. (1997). Nonaffine deformation and elasticity of polymer networks. *Macromolecules, 30*(25), 8036–8044.

Shi, H. (2001). Introducing natural antioxidants. In J. Pokorny, N. Yanishlieva, & M. Gordon (Eds.), *Antioxidants in foods. Practical applications*. Cambridge, England: CRC Press. Woodhead Publishing Limited. (Chapter 8).

Skendi, A., Biliaderis, C. G., Lazaridou, A., & Izydorczyk, M. S. (2003). Structure and rheological properties of water soluble β-glucans from oat cultivars of *Avena sativa* and *Avena bysantina*. *Journal of Cereal Science, 38*, 15–31.

Sokal, R. R., & Rohlf, F. J. (1995). *Biometry. The principles and practice of statistics in biological research*. San Francisco, U.S.A.: W.H. Freeman and Co. Publisher.

Tang, J., Lelievre, J., Tung, M. A., & Zeng, Y. (1994). Polymer and ion concentration effects on gellan gel strength and strain. *Journal of Food Science, 59*(1), 216–220.

Treloar, L. R. G. (1958). *The physics of rubber elasticity*. Amen House, London, UK: Oxford University Press.

Vittadini, E., Dickinson, L. C., & Chinachoti, P. (2001). ^{1}H and ^{2}H NMR mobility in cellulose. *Carbohydrate Polymers, 46*(1), 49–57.

Xu, X., Liu, W., & Zhang, L. (2006). Rheological behavior of Aeromonas gum in aqueous solutions. *Food Hydrocolloids, 20*, 723.6–729.6.

Yang, L., & Paulson, A. T. (2000). Mechanical properties of water vapour barrier properties of edible gellan films. *Food Research International, 33*, 563–570.